Emergent Critical Charge Fluctuations at the Kondo Breakdown of Heavy Fermions

Yashar Komijani and Piers Coleman

Phys. Rev. Lett. **122**, 217001 — Published 28 May 2019

DOI: 10.1103/PhysRevLett.122.217001

Emergent critical charge fluctuations at the Kondo break-down of Heavy Fermions

Yashar Komijani[1] and Piers Coleman[1,2]

[1]*Department of Physics and Astronomy, Rutgers University, Piscataway, New Jersey, 08854, USA*
[2]*Department of Physics, Royal Holloway, University of London, Egham, Surrey TW20 0EX, UK*

(Dated: May 2, 2019)

One of the challenges in strongly correlated electron systems, is to understand the anomalous electronic behavior that develops at an antiferromagnetic quantum critical point (QCP), a phenomenon that has been extensively studied in heavy fermion materials. Current theories have focused on the critical spin fluctuations and associated break-down of the Kondo effect. Here we argue that the abrupt change in Fermi surface volume that accompanies heavy fermion criticality leads to critical charge fluctuations. Using a model one dimensional Kondo lattice in which each moment is connected to a separate conduction bath, we show a Kondo breakdown transition develops between a heavy Fermi liquid and a gapped spin liquid via a QCP with ω/T scaling, which features a critical charge mode directly associated with the break-up of Kondo singlets. We discuss the possible implications of this emergent charge mode for experiment.

Introduction - The relation between valence fluctuations and the Kondo effect has long fascinated the physics community [1]. A partially occupied atomic state, weakly hybridized with a conduction sea, forms a local moment [2] and its virtual valence fluctuations give rise to low frequency spin-fluctuations, while leaving its charge essentially frozen. On the other hand, in heavy fermion systems, the Kondo-screening of the local moments gives rise to an enlargement of the Fermi surface, a phenomenon that is well established both theoretically [3, 4] and through Hall coefficient [5], quantum oscillation [6], ARPES and STM measurements [7, 8]. The large Fermi surface of a Kondo lattice is believed to partially collapse when Kondo screening is disrupted [9–16] at an antiferromagnetic (AFM) quantum critical point (QCP), a phenomenon known as "Kondo breakdown" (KBD).

Recently, a number of experiments have observed a coincidence of critical charge fluctuations at the magnetic quantum critical points in $CeRhIn_5$ [17] $YbRh_2Si_2$ [18] and β-$YbAlB_4$ [19]. Watanabe and Miyake have argued that the development of soft charge fluctuations near a heavy fermion QCP is likely a result of a quantum-critical end-point, in which a first-order valence changing transition line is suppressed to low temperatures [20–24]. Here we present an alternative view, arguing that the coincidence of soft charge fluctuations and Kondo breakdown is a natural consequence of the Fermi surface collapse.

In the eighties, Anderson introduced the concept of a *nominal valence* to distinguish the valence of a rare earth ion infered from the apparent delocalization of f-electrons [25, 26], from the core-level valence, infered from spectroscopy. From this perspective, a shift in nominal valence is associated with formation of a large Fermi surface, even in a strict Kondo lattice where the core-level valence is fixed. Interpreted literally, this implies a kind of many-body *ionization* in the Kondo lattice, in which a fractionalization of local moments into charged heavy electrons, leaves behind a compensating positive background of Kondo singlets [27]. Taken to its logical extreme, such an interpretation would then imply that at KBD quantum critical point, degenerate fluctuations in the nominal valence will give rise to an observable soft charge mode.

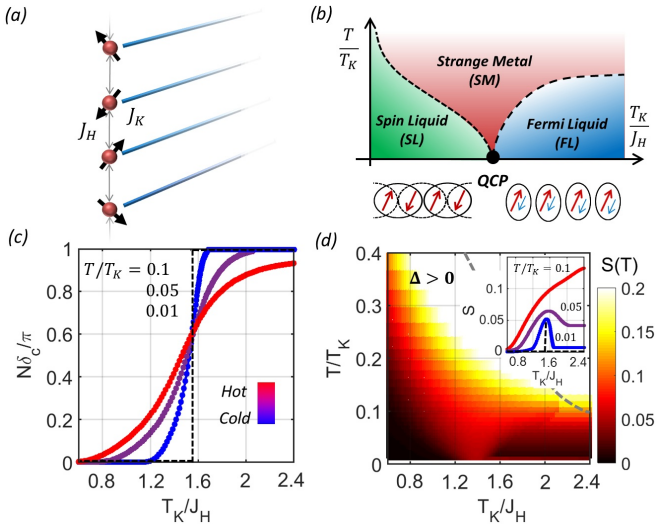

FIG. 1. (color online) (a) Model 1D Kondo lattice, with local moments (red) with an AFM Heisenberg coupling J_H, individually screened by separate conduction electron baths (blue wires). (b) Schematic phase diagram showing the transition between heavy-Fermi liquid (FL) and spin-liquid (SL) phases at a QCP which evolves to a fan of strange metal (SM) at finite temperature. (c) Conduction electron phase shift δ_c as a function of T_K/J_H, which extrapolates to a step-like jump from 0 to π/N as $T \to 0$. (d) Color map of entropy $S(T)$, showing the collapse of energy scales at the QCP: the dashed line separates localized ($\Delta = 0$ to the right) and delocalized ($\Delta > 0$ to the left) spinon regimes. Inset: temperature cuts showing the accumulation of entropy at the QCP.

While Kondo Breakdown has been extensively modelled at an impurity-level [28, 29] and simulated using dynamical mean-field theory [10, 30, 31], a possible link with charge fluctuations has not sofar been explored in the lattice. To examine this idea, we introduce a simple field-theoretic framework for Kondo breakdown, emplying a Schwinger boson representation of spins that permits us to treat Kondo screening and antiferromagnetism [32, 33]. Early application of this method demonstrated its efficacy for describing a ferromagnetic quantum critical point [34] in a Kondo lattice. Here

we consider a Kondo screened one dimensional (1D) AFM [Fig. 1a], examining the quantum phase transition transition between a spin-liquid and a Fermi liquid [Fig. 1(b)]. The conduction electron phase shift (related to the Fermi surface size) jumps at $T = 0$, indicating that QCP is a KBD transition. Additionally, we find that the KBD features a zero point entropy [Fig. 1(d)]. In our calculations we observe that the KBD is linked to the emergence of a gapless charge degree of freedom at the QCP which occurs in natural coincidence with a divergent charge and staggered spin susceptibility.

The simplified 1D Kondo lattice is a chain of antiferromagnetically coupled spins each individually screened by a conduction electron bath:

$$H = \sum_j \Big[H_C(j) + J_K \vec{S}_j \cdot \vec{\sigma}_j + J_H \vec{S}_j \cdot \vec{S}_{j+1} \Big]. \quad (1)$$

Here $\vec{S}_j$ is the spin at the j-th site, coupled antiferromagnetically to its neigbor with strength J_H. $H_C(j) = \sum_{\mathbf{p}} \epsilon_{\mathbf{p}} c^\dagger_{\mathbf{p}\alpha}(j) c_{\mathbf{p}\alpha}(j)$ describes the conduction bath coupled to the j-th moment in the chain, where $\mathbf{p}$ is the momentum of the conduction electron. $\vec{\sigma}_j = \psi^\dagger_{j\alpha} \vec{\sigma}_{\alpha\beta} \psi_{j\beta}$ is the spin density at site j, where $\psi^\dagger_{j\alpha} = \sum_{\mathbf{p}} c^\dagger_{\mathbf{p}\alpha}(j)$ creates an electron on the chain at site j.

Global phase diagram - Numerical and experimental studies of heavy-fermion systems are often interpreted [10, 35, 36] within a global phase diagram of the Kondo lattice, with two axes: a Doniach parameter $x = T_K/J_H$ [37], where T_K is the Kondo temperature, and a frustration parameter y representing the magnitude of quantum fluctuations, controlled by geometrical or dimensional frustration. The 1D limit provides a way to explore the two extremes of y: on the one hand, the uniform magnetization of a 1D FM commutes with the Hamiltonian and has no quantum fluctuations, corresponding to $y = 0$ [34], whereas a 1D AFM never develops long range order, loosely corresponding to $y = \infty$. When the magnetic coupling is Ising-like, both models can be mapped to the dissipative transverse-field Ising model. But a Heisenberg magnetic coupling has been proven to be difficult to treat with these methods [38, 39] and a single formalism that can access various phases and critical points is highly desirable.

The method is a large-N approach, obtained by enlarging the spin rotation group from SU(2) to SP(N), representing the spin S local moments using Schwinger bosons ("spinons"), according to $S_{\alpha\beta} = b^\dagger_\alpha b_\beta - \tilde{\alpha}\tilde{\beta} b^\dagger_{-\beta} b_{-\alpha}$[40, 41], where $\alpha \in [\pm 1, \cdots \pm N/2]$, $\tilde{\alpha} = \mathrm{sign}(\alpha)$ and $n_b(j) = 2S$ is the number of bosons per site. Each moment is coupled to a K-channel conduction sea, with Hamiltonian

$$H = \sum_j \Big[H_{AFM}(j) + H_K(j) + H_C(j) + H_\lambda(j) \Big], \quad (2)$$

where

$$\begin{aligned} H_{AFM}(j) &= -(J_H/N)(\tilde{\alpha} b^\dagger_{j\alpha} b^\dagger_{j+1,-\alpha})(\tilde{\beta} b_{j+1,-\beta} b_{j\beta}), \\ H_K(j) &= -(J_K/N)\big(b^\dagger_{j\alpha} \psi_{ja\alpha}\big)\big(\psi^\dagger_{ja\beta} b_{j\beta}\big), \\ H_\lambda(j) &= \lambda_j [n_b(j) - 2S]. \end{aligned} \quad (3)$$

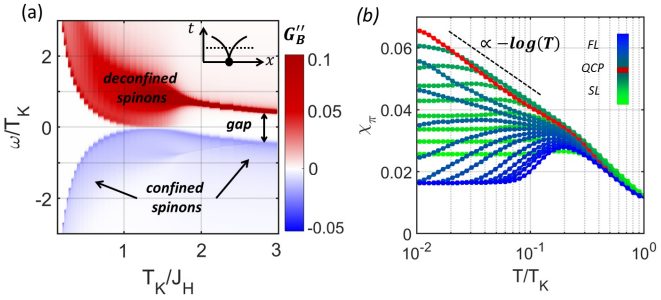

FIG. 2. (color online) (a) Calculated spectral function of spinons $G''_B(\omega - i\eta)$ at $T/T_K = 0.03$ shows confined spinons protected by a gap in the FL and SL, and deconfined with with a soft excitation gap in the SM regime. (b) Staggered spin susceptibilities vs. T/T_K for various various values of T_K/J_H from SL (in green) and FL (in blue) passing QCP (in red). A log-divergence at the QCP is visible.

Here we have adopted a summation convention for the repeated greek $\alpha \in [\pm 1, \pm N/2]$ spin and roman $a \in [1, K]$ channel indices. The Lagrange multiplier λ_j imposes the constraint $n_b(j) = 2S$: we take $2S = K = 2sN$ for perfect screening, where s is kept fixed.

We carry out the Hubbard-Stratonovich transformations:

$$\begin{aligned} H_K(j) &\to \big[(b^\dagger_{j\alpha} \psi_{ja\alpha}) \chi_{ja} + \mathrm{h.c}\big] + \frac{N \bar{\chi}_{ja} \chi_{ja}}{J_K} \\ H_{AFM}(j) &\to \big[\bar{\Delta}_j (\tilde{\alpha} b^\dagger_{j+1,-\alpha} b^\dagger_{j,\alpha}) + \mathrm{h.c}\big] + \frac{N|\Delta_j|^2}{J_H}, \end{aligned} \quad (4)$$

where χ_{ja} is a Grassmanian "holon" field that mediates the Kondo effect at site j in channel a, while Δ_j describes the development of singlets between site j and $j+1$. See [34] For a discussion of spurious 1st order transition and their remedy.

A mean-field RVB description of the 1D magnetism is obtained from a uniform mean-field theory where $\Delta_j = i\Delta_B/2$, and $\lambda_j = \lambda$, giving rise to a bare spinon dispersion $\epsilon_B(p) = [\lambda^2 - \Delta_p^2]^{\frac{1}{2}}$, with $\Delta_p = \Delta_B \sin p$. Both b and χ fields have non-trivial dynamics [32, 34, 42–44], with self-energies

$$\Sigma_\chi(\tau) = g_0(-\tau) G_B(\tau), \qquad \Sigma_B(\tau) = -\gamma g_0(\tau) G_\chi(\tau). \quad (5)$$

Here, $\gamma = K/N = 2s$ and $G_\chi(\tau)$, $G_B(\tau)$ and $g(\tau)$ are the local propagators of the holons, spinons and conduction electrons, respectively. The conduction electron self-energy is of order $\mathcal{O}(1/N)$ and is neglected in the large-N limit, so that $g_0(\tau)$ is the bare local conduction electron propagator. The holon Green's function $G_\chi(z) = [-{J_K}^{-1} - \Sigma_\chi(z)]^{-1}$, is purely local, whereas the spinons are delocalized by the RVB pairing with propagator $\mathbb{G}_B(p,z) = [z\tau^z - \lambda \mathbb{1} - \Delta_p \tau^x - \mathbb{\Sigma}_B(z)]^{-1}$. The self-energy $-\mathbb{\Sigma}_B(z)$ is diagonal in Nambu space, while the momentum sum in $\mathbb{G}^{\mathrm{loc}}_B(z) = \sum_p \mathbb{G}_B(p,z)$ can be done analytically [45].

Stationarity of the free energy with respect to λ enforces the mean-field constraint $\langle n_b(j) \rangle = K$, and with respect to Δ_B determines the relation $\Delta_B(J_H)$ [45]. We solve these self-consistent equations numerically on the real-frequency axis using linear and logarithmic grids.

The two limits - In absence of Kondo screening (when T_K/J_H is small) the constraint is satisfied with $\lambda > \Delta_B$. This Schwinger boson model describes a bipartite spin chain, in which each sublattice is in the symmetric spin-S representation of SP(N) [40, 41]: Each spin can form singlets with its neighbors in an RVB state for any value S. This, together with the Gutzwiller projection treated by a soft constraint leads to a U(1) gapped spin liquid [33], closely analogous to the integer-spin Haldane chain [46]. A lattice with closed boundary condition has a unique ground state and corresponds to a symmetry protected topological phase [47].

The large T_K/J_H limit corresponds to a local Fermi liquid [34, 44] at each site of the chain, in which the electrons and spinons form bound, localized singlets, protected by a spectral gap of the size T_K; the remaining electrons are scattered with a phase shift $\delta_c = \pi/N$. Fig. (1b) summarizes the phase diagram as T_K/J_H is varied between the above two limits, which we discuss in the following.

Ward identity, Entropy, Phase Shifts - At large N, the many body equations can be derived from a Luttinger Ward functional, leading to an exact relation between the conduction electron and holon phase shifts $\delta_c = \delta_\chi/N$ and a closed form formula for the entropy [43, 44]. Fig. 1(c) shows the conduction electron phase shift $N\delta_c/\pi$ as a function of T_K/J_H. In the Fermi liquid, $\delta_\chi = N\delta_c$ is equal to π, equivalent to a large Fermi surface, but it is zero in the spin liquid regime. Extrapolating the calculations to $T \to 0$, the phase shift appears to jump at the QCP separating the spin-liquid (decoupled electrons) and the Fermi-liquid. From the perspective of conduction electrons, both SL and FL phases are Fermi liquids and the transition in δ_χ is a measure of change in the Fermi surface, a manifestation of Kondo breakdown (KBD).

Entropy - Fig. 1(d) shows the colormap of the entropy $S(T)$ across the phase diagram. The gray dashed line indicates a second order phase transition for the internal variable Δ_B that separates a local Fermi liquid ($\Delta_B = 0$) from a delocalized regime ($\Delta_B > 0$). The collapse of the energy scale from both sides are visible. Unlike the 1D ferromagnetic QCP [34], the antiferromagnetic QCP develops a residual entropy $S_E/N \approx 1/20$ at a spin of $s = 0.1$ per moment (inset of Fig. 1d),

Magnetic excitations - Fig. (2a) shows the spinon spectrum $G''_B(\omega - i\delta)$ vs. T_K/J_H at $T/T_K = 0.03$. Approaching the transition from the Fermi liquid side (right), the spinon spectrum shifts to positive frequencies and, maintaining overall gap size, brings the gap edge close to the chemical potential and only then, the hard gap closes at the QCP. Passing through the critical point, the gap re-opens due to development of short-range RVBs in the spin liquid regime. Fig. 2(b) shows the temperature dependence of the staggered spin susceptibility χ_π, which acquires a logarithmic temperature dependence $\chi_\pi \sim -\log T$ at the QCP. The Fermi liquid (blue) exhibits a crossover from Curie law $1/T$ to a Pauli form $1/T_K$, with a characteristic peak at $T/T_K \sim 0.1$. As T_K/J_H is reduced the peak position is unchanged (unlike the 1D FM case [34]) whereas the low temperature susceptibility develops a logarithmic divergence. Similar divergence is observed in local spin susceptibility but the uniform susceptibility is only suppressed by magnetism [45].

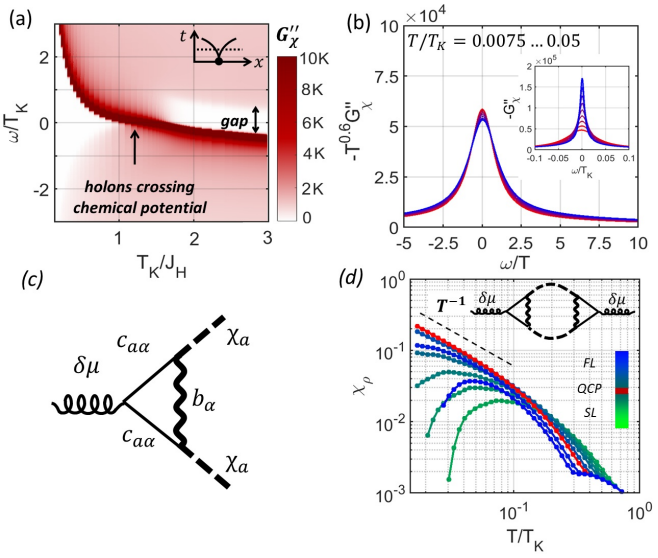

FIG. 3. (a) Calculated spectrum of holons $G''_\chi(\omega - i\eta)$ showing that the holon mode crosses the chemical potential at the QCP. (b) ω/T scaling of the holon Green's function $G''_\chi(\omega - i\eta)$ at the QCP. The inset shows the holon mode before scaling. (c) The $\mathcal{O}(1)$ charge vertex of holons coupling them to potential fluctuations. (d) The charge susceptibility computed via this vertex corrections (inset) shows a T^{-1} divergence at the QCP point (red) and its suppression in SL/FL sides.

The holon spectrum - $G''_\chi(\omega - i\eta)$ shows a striking behavior at the QCP (Fig. 3a). Most of the spectral weight is contained in a sharp holon mode which crosses the chemical potential as T_K/J_H is tuned from Fermi liquid (right) to spin-liquid (left). In the critical regime at a finite temperature, the holon mode is pinned to the Fermi energy over a finite range of Doniach parameter, which shrinks to a point as $T \to 0$, forming a strange metal (SM) regime at finite temperature with deconfined critical holon and spinon modes.

ω/T scaling - At the QCP, the holon mode lies at zero energy. Fig. 3(b) shows that the holon spectra at different temperatures collapse onto a single scaling curve $G''_\chi(\omega, T) = T^{-\alpha} f(\omega/T)$. For $s = 0.1$ we find $\alpha = 0.6$ consistent with a scaling analysis [45]. The universality class of the QCP appears to be that of an overscreened impurity model[32] , with an effective number of channels $K_{\rm eff}/N = (1/\alpha - 1) \approx 0.67 > 2s$.

The holon modes have an emergent coupling to the electromagnetic field, mediated via the internal vertices of the lattice Kondo effect. In particular, the field theory implies an $\mathcal{O}(1)$ vertex correction that couples to the electric potential as shown in Fig. 3(c). At low energies the vertex can be approximated by $\Gamma_\chi = -\frac{d}{d\omega}\Sigma_\chi$. This quantity perfectly cancels the wavefunction renormalization of the holon propagator $G_\chi \approx Z_\chi/\omega$, where $Z_\chi = -[\partial_\omega \Sigma_\chi]^{-1}$, so that the holon couples to the electric potential with a net charge $\Gamma_\chi Z_\chi = +1$.

Fig. (3)(d) shows the charge susceptibility calculated using this vertex corrections. At the QCP, the temperature dependence of the holon charge susceptibilty acquires a Curie-like temperature dependence $\chi_\rho \sim 1/T$.

Discussion - We have studied a simplified Kondo lattice model in the large-N limit, enabling us to extract the KBD physics directly on a lattice. It is illuminating to note that both specific heat and spin susceptibility [45] disagree with the predictions of Hertz-Millis theories of the KBD based on using hybridization as an order parameter [14, 15].

One of the striking features of our description of the KBD quantum critical point is the presence of an emergent, spinless critical charge mode with a Curie-like charge susceptibility. Our model calculations can be extended in various ways, by going to higher dimensions, by generalizing to the mixed valence regime, and with considerable increase in computation, to a model in which a single bath is shared between all moments. In the general Kondo lattice, the charge conservation Ward identity links the change in the volume of the conduction electron Fermi surface Δv_{FS} to the charge density of the Kondo singlets, described by the holon phase shift [43]

$$N\frac{\Delta v_{FS}}{(2\pi)^3} = \overbrace{\sum_{\mathbf{p}} \frac{1}{\pi}\mathrm{Im}\ln\Big[-G_\chi^{-1}(\mathbf{p},z)\Big]_{z=0+i\delta}}^{\delta_\chi/\pi} \qquad (6)$$

Quite generally, the holon phase shift is zero or π in the localized magnetic, or Fermi liquid phases respectively, but must jump between these two limits at the quantum critical point establishing critical holons. This and the O(1) charge vertex leads to critical charge fluctuations, independent of the details of the model. This strongly suggests that the gapless holon excitions seen in our model calculation will persist at a more general Kondo breakdown quantum critical fixed point. Whether the Ward identity remains valid in models with reduced symmetry, is something we leave for future.

This raises the fascinating question how the predicted critical charge modes at KBD might be observed experimentally. One mode of observation, is via the coupling to nuclear Mossbauer lines [48]. A recent observation of the splitting of the Mossbaüer line-shape [19], characteristic of slow valence fluctuations, may be a fingerprint of these slow charge fluctuation.

Another interesting question is whether the residual entropy of the QCP might survive beyond the independent bath approximation. A residual ground-state entropy is a signature of infinite-range entanglement, and has been seen in various quantum models, such as the two channel Kondo model [49–51] or the SYK model [52–54]. In the single-channel Kondo problem, the Kondo screening length [55] $\xi_K \sim v_F/T_K^{\rm eff}$ plays the role of an entanglement length-scale, beyond which the singlet ground-state is disentangled from the conduction sea. If the collapse of the Kondo temperature $T_K^{\rm eff} \to 0$ at the QCP of a Kondo lattice involves a divergence of the entanglement length $\xi_K \to \infty$, the corresponding quantum critical point would be expected to exhibit an extensive entanglement entropy. Such naked quantum criticality is likely to be censored by competing ordered phases that consume the entanglement entropy of the critical regime, concealing QCP beneath a dome of competing phase, such as superconductivity.

Lastly, a peculiar feature of strange metals in heavy-fermions is that the resistivity tends to be linear in T over a wide range of tempreature. In quenched disordered models it is possible [56] to derive such behavior from model calculations. One of the fascinating implications of a Curie-law charge susceptibility $\chi_\rho \sim 1/T$ seen in our calculations, is that if combined with a temperature-independent diffusion of incoherent holon motion, it would give rise to a Curie conductivity (linear resistivity $\rho \propto 1/\sigma \sim T$) via the Einstein relation $\sigma = D\chi_c \sim 1/T$, where D is the holon diffusion constant. This raises the interesting possibility that linear resistivities are driven by an emergent critical charge mode.

This work was supported by NSF grant DMR-1309929 (Piers Coleman) in its early stages, and by a Rutgers University Materials Theory postdoctoral fellowhsip (Yashar Komijani). We would like to thank S. Nakatsuji, H. Kobayashi, A. Vishwanath, J. Pixley, C. Chung and A. Georges for stimulating discussions, M. Oshikawa for helpful correspondence and A. M. Lobos, M. A. Cazalilla and P. Chudzinski for discussing that clarified the relation to [38, 39].

[1] J. R. Schrieffer and P. A. Wolff, Phys. Rev. **149**, 491 (1966).
[2] P. W. Anderson, Rev. Mod. Phys. **50**, 191 (1978).
[3] M. Yamanaka, M. Oshikawa, and I. Affleck, Phys. Rev. Lett. **79**, 1110 (1997).
[4] M. Oshikawa, Phys. Rev. Lett. **84**, 3370 (2000).
[5] S. Paschen, T. Lühmann, S. Wirth, P. Gegenwart, O. Trovarelli, C. Geibel, F. Steglich, P. Coleman, and Q. Si, Nature **432**, 881 (2004).
[6] H. Shishido, R. Settai, H. Harima, and Y. Onuki, Journal of the Physical Society of Japan **74**, 1103 (2005).
[7] Q. Y. Chen, D. F. Xu, X. H. Niu, J. Jiang, R. Peng, H. C. Xu, C. H. P. Wen, Z. F. Ding, K. Huang, L. Shu, Y. J. Zhang, H. Lee, V. N. Strocov, M. Shi, F. Bisti, T. Schmitt, Y. B. Huang, P. Dudin, X. C. Lai, S. Kirchner, H. Q. Yuan, and D. L. Feng, Phys. Rev. B **96**, 045107 (2017).
[8] P. Aynajian, E. H. da Silva Neto, A. Gyenis, R. E. Baumbach, J. D. Thompson, Z. Fisk, E. D. Bauer, and A. Yazdani, Nature **486**, 201 (2012).
[9] P. Coleman, C. Pepin, Q. Si, and R. Ramazashvili, J. Phys. Condens. Matter **13**, R723 (2001).
[10] Q. Si, S. Rabello, K. Ingersent, and J. L. Smith, Nature **413**, 804 (2001).
[11] T. Senthil, S. Sachdev, and M. Vojta, Phys. Rev. Lett. **90**, 216403 (2003).
[12] T. Senthil, M. Vojta, and S. Sachdev, Phys. Rev. B **69**, 035111 (2004).
[13] P. Coleman, J. B. Marston, and A. J. Schofield, Phys. Rev. B **72**, 245111 (2005).
[14] I. Paul, C. Pépin, and M. R. Norman, Phys. Rev. Lett. **98**, 026402 (2007).
[15] C. Pépin, Phys. Rev. Lett. **98**, 206401 (2007).
[16] A. Nejati, K. Ballmann, and J. Kroha, Phys. Rev. Lett. **118**,

117204 (2017).
[17] Z. Ren, G. W. Scheerer, D. Aoki, K. Miyake, S. Watanabe, and D. Jaccard, Phys. Rev. B **96**, 184524 (2017).
[18] L. Prochaska, X. Li, D. C. MacFarland, A. M. Andrews, M. Bonta, E. F. Bianco, S. Yazdi, W. Schrenk, H. Detz, A. Limbeck, Q. Si, E. Ringe, G. Strasser, J. Kono, and S. Paschen, arxiv: 1808.02296 (2018). (2018).
[19] H. Kobayashi, Y. Sakaguchi, M. Oura, S. Ikeda, K. Kuga, S. Nakatsuji, R. Masuda, Y. Kobayashi, M. Seto, Y. Yoda, Y. Komijani, P. Chandra, and P. Coleman, to be submitted (2018).
[20] S. Watanabe and K. Miyake, J. Phys. Soc. Jpn. **82**, 083704 (2013).
[21] K. Miyake and S. Watanabe, J. Phys. Soc. Jpn. **83**, 061006 (2014).
[22] S. Watanabe and K. Miyake, Journal of the Physical Society of Japan **83**, 103708 (2014).
[23] S. Watanabe and K. Miyake, Journal of Physics: Conference Series **592**, 012087 (2015).
[24] G. W. Scheerer, Z. Ren, S. Watanabe, G. Lapertot, D. Aoki, D. Jaccard, and K. Miyake, npj Quantum Materials , 1 (2018).
[25] P. W. Anderson, in Moment Formation in Solids, edited by W. J. L. Buyers (Plenum, New York, 1983) pp. 313–326.
[26] G. Aeppli and Z. Fisk, Comm. Condens. Matter Phys. **16**, 155 (1992).
[27] E. Lebanon and P. Coleman, Physica B: Condensed Matter **403**, 1194 (2008).
[28] J. H. Pixley, S. Kirchner, K. Ingersent, and Q. Si, Phys. Rev. Lett. **109**, 086403 (2012).
[29] T. Chowdhury and K. Ingersent, Phys. Rev. B **91**, 035118 (2015).
[30] L. De Leo, M. Civelli, and G. Kotliar, Phys. Rev. Lett. **101**, 256404 (2008).
[31] L. C. Martin, M. Bercx, and F. F. Assaad, Phys. Rev. B **82**, 245105 (2010).
[32] O. Parcollet and A. Georges, Phys. Rev. Lett. **79**, 4665 (1997).
[33] D. P. Arovas and A. Auerbach, Phys. Rev. B **38**, 316 (1988).
[34] Y. Komijani and P. Coleman, Phys. Rev. Lett. **120**, 157206 (2018).
[35] P. Coleman, C. Pèpin, Q. Si, and R. Ramazashvili, Journal of Physics: Condensed Matter **13**, R723 (2001).
[36] P. Coleman and A. H. Nevidomskyy, Journal of Low Temperature Physics **161**, 182 (2010).
[37] S. Doniach, Physica B+C **91**, 231 (1977).
[38] A. M. Lobos, M. A. Cazalilla, and P. Chudzinski, Phys. Rev. B **86**, 035455 (2012).
[39] A. M. Lobos and M. A. Cazalilla, Journal of Physics: Condensed Matter **25**, 094008 (2013).
[40] N. Read and S. Sachdev, Phys. Rev. Lett. **66**, 1773 (1991).
[41] R. Flint and P. Coleman, Phys. Rev. B **79**, 014424 (2009).
[42] O. Parcollet, A. Georges, G. Kotliar, and A. Sengupta, Phys. Rev. B **58**, 3794 (1998).
[43] P. Coleman, I. Paul, and J. Rech, Phys. Rev. B **72**, 094430 (2005).
[44] J. Rech, P. Coleman, G. Zarand, and O. Parcollet, Phys. Rev. Lett. **96**, 016601 (2006).
[45] See supplementary material.
[46] F. D. M. Haldane, Phys. Rev. Lett. **50**, 1153 (1983).
[47] F. Pollmann, A. M. Turner, E. Berg, and M. Oshikawa, Phys. Rev. B **81**, 064439 (2010).
[48] Y. Komijani and P. Coleman, Phys. Rev. B **94**, 085113 (2016).
[49] N. Andrei and C. Destri, Physical Review Letters **52**, 364 (1984).
[50] A. M. Tsvelik and P. B. Wiegmann, Zeitschrift für Physik B Condensed Matter **54**, 201 (1984).
[51] A. W. Ludwig and I. Affleck, Nuclear Physics B **428**, 545 (1994).
[52] S. Sachdev and J. Ye, Phys. Rev. Lett. **69**, 2411 (1992).
[53] A. Georges, O. Parcollet, and S. Sachdev, Phys. Rev. B **63**, 134406 (2001).
[54] J. Maldacena and D. Stanford, Phys. Rev. D **94**, 106002 (2016).
[55] I. Affleck, in Perspectives of Mesoscopic Physics, edited by A. Aharony and E.-W. Ora (World Scientific, 2010) pp. 1–44, 0911.2209.
[56] O. Parcollet and A. Georges, Phys. Rev. B **59**, 5341 (1999).